A hybrid Machine Learning unmixing method for gamma-spectrometry

1st Dinh Triem Phan
Université Paris-Saclay, List CEA
Palaiseau, France
dinh-triem.phan@cea.fr

2nd Jérôme Bobin
Université Paris-Saclay, Irfu CEA
Gif-sur-Yvette, France
jerome.bobin@cea.fr

3rd Cheick Thiam
Université Paris-Saclay, List CEA
Palaiseau, France
cheick.thiam@cea.fr

4th Christophe Bobin
Université Paris-Saclay, List CEA
Palaiseau, France
christophe.bobin@cea.fr

***Abstract*—The automatic identification and quantification of gamma-emitting radionuclides, accounting for spectral deformation due to gamma interactions in the environment of radioactive sources, is a challenge for various nuclear applications. In this paper, this problem is addressed by developing a hybrid approach combining Machine Learning and classical statistical methods. A specific Machine Learning-based autoencoder that can capture spectral variability with limited data is proposed. A novel hybrid unmixing algorithm employing a pre-trained autoencoder is investigated for joint estimation of spectral signatures and counting in the case of mixtures of four radionuclides (^{57}Co, ^{60}Co, ^{133}Ba, ^{137}Cs). This study was carried out to take account of spectral deformation due to attenuation and Compton scattering at low statistics. The results demonstrate the validity of this new hybrid approach based on Machine Learning and Maximum Likelihood for the automatic full-spectrum analysis of gamma-spectra.**

***Index Terms*—Gamma-ray spectrometry, Spectral variability, Hybrid algorithm, Machine Learning, Interpolating autoencoder, Semi-blind unmixing**

I. Introduction

γ-ray spectrometry is a classical technique allowing the identification and quantification of γ-emitting radionuclides in many fields of nuclear applications such as fast spectroscopic identification for environmental measurements (e.g., following a radiological or nuclear accident), decommissioning of nuclear facilities or security screening.

Mathematically, an observed spectrum $y = [y_1, ..., y_M]$ is a vector of M channels, with each channel representing energy intervals registered by a detector sensitive to γ-photons. For each channel m, the counting y_m is the number of events that the deposited energy fell within that interval. The observed spectrum y follows the Poisson distribution of Xa : $y \sim \mathcal{P}(Xa)$ where X is a matrix composed of the normalized spectral signature of all radionuclides (including the natural background (Bkg)) and a is the vector containing the counting or mixing weights of each radionuclide. The spectral unmixing is the inverse problem which estimates the counting a from the observed spectrum y and the spectral signatures X. This problem can be solved by the statistical approach based on the Maximum Likelihood Estimation (MLE) [1] [2].

In real-life applications, a complex environment can lead to the variability of experimental γ-spectra. Indeed, the shape of γ-spectra may vary due to physical phenomena such as Compton scattering, attenuation or fluorescence due to photon interactions surrounding radioactive sources. For instance, when a radioactive point source is placed in a steel sphere and the steel thickness varies from 0.001 mm to 30 mm, the spectral signatures of all radionuclides also vary (see Fig. 1). In this case, the spectral signature matrix X is not fixed and known, so we have to jointly estimate X and a from y and the spectral variability information. As a result, our problem is related to semi-blind source separation.

Although the attenuation phenomenon is mentioned in a few papers ([3], [4]), the current state-of-the-art of γ-ray spectrometry approaches are insufficient to deal with spectral variability, mixing model and Poisson statistics, especially at low-statistics. For this purpose, this paper presents a novel hybrid unmixing method that combines a standard MLE-based statistical approach with a Machine learning (ML)-based model, coined Interpolating AutoEncoder (IAE), to capture spectral signature variability using Geant4 simulated spectral signatures [5].

The article is organized as follows:

- The IAE model is described in Section II. Two approaches to modeling γ-spectrum deformations are presented: an individual model that learns for each radionuclide independently and a joint model for all radionuclides.
- A novel hybrid ML unmixing algorithm to estimate spectral signatures and mixing weights is presented in Section III. It is based on a Block coordinate descent (BCD) minimization scheme, employing the IAE model as a constraint on spectral signatures.

II. Interpolating autoencoder: modeling of spectral signatures

A. IAE: a trainable model to account for the spectral signature deformations

The aim is to construct a surrogate model to describe spectral signature deformations parameterized by sphere thickness. Mathematically, for each radionuclide, the spectral signatures are signals that live on a one-dimensional manifold representing the relationship between thickness and the resulting spectral signature. Since no analytical model is available, this

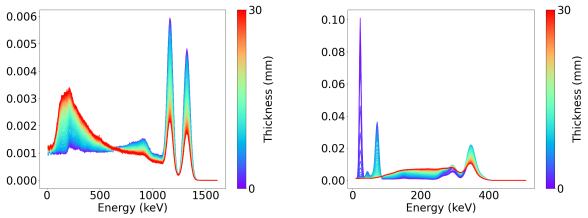

Fig. 1. Simulated spectral signatures of ^{60}Co (left) and ^{133}Ba (right) as a function of steel thickness. The y-axis represents normalized amplitudes. The blue curves correspond to low thicknesses and the red curves correspond to high thicknesses.

paper proposes using an ML approach to learn the manifold mentioned above.

In the ML literature, autoencoders are used to learn a surrogate model for signals that live on a low-dimensional manifold. One of the main requirements of standard autoencoders is the need for a large amount of training data. However, simulating spectral signatures with Geant4 is costly in computation, restricting the number of samples available for training ML model. To overcome this bottleneck, we make use of the IAE presented in [6]. In a nutshell, the IAE consists of an additional element that performs linear interpolation from anchor points in the latent domain. The advantage of IAE is that it forces samples to be described as interpolants of anchor points that are known to be on the physical manifold that describes the spectral signature deformations. In practice, the IAE is a neural network with the architecture described in Fig. 2.

Once the model has been learned, the IAE can be used as a generative model. The input sample can be estimated as decoding of a linear interpolation of the encoded anchor points. In other words, the sample domain $\mathcal{M}$ can be approximated as a domain generated by a known function of a latent variable λ: $\mathcal{M} \approx \{\Psi(\mathbf{\Omega}\lambda); \lambda \in S_d\}$ where S_d represents the simplex space: $\lambda \in S_d$ means that the sum of λ equals one. Consequently, the spectral signatures can be modeled via very low-dimensional variables for our application.

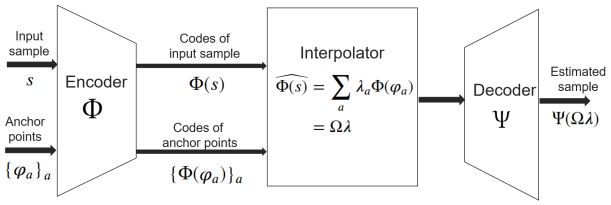

Fig. 2. Diagram of IAE

B. Individual IAE-based spectral signature model

In this section, a different IAE model is trained independently for each radionuclide. The architecture of the IAE model is defined based on the encoder and decoder architectures, as well as the choice and number of anchor points, which limit the dimensionality of the model. Mathematically, the number of anchor points depends on the actual dimension of the physical manifold that represents the spectral variability. As the spectral deformations depend only on the sphere thickness, they are characterized by a single parameter. As specified in [6], the number of anchor points must be at least 2 (due to the simplex constraint).

Several types of neural networks such as MLP or CNN have been studied for building IAE models, and in our case, CNN more effectively captures the structure and variability of spectral signatures. Consequently, the encoder and decoder architecture in the present work is based on CNN. More specifically, the encoder and decoder consist of L layers: each contains a 1D convolution layer to obtain useful information, batch normalization to speed up learning and make it more stable and an Elu activation function. The general structure of the IAE is the same for all radionuclides. However, the number of filters, filter size and stride in each layer are different. Various hyperparameter values were studied and the best hyperparameters were chosen for each IAE model associated with each radionuclide.

C. Joint IAE-based spectral signature model

A more realistic case involving several radionuclides placed in the same source housing has been studied. In this configuration, all radionuclides have the same sphere thickness and material, so the spectral signatures of all radionuclides are correlated. Since the IAE model is trained to capture spectral variability, the latent domain describes how they evolve as thickness changes. In this context, only one IAE model is required to encode this information in a single common latent domain for all radionuclides. Consequently, the previous IAE model is extended to be trained simultaneously for all radionuclides to share the same latent space. This means that the same λ parameter can be used to represent all spectral signatures at once. This modification is particularly advantageous since it enables the accounting of correlations between spectral signature deformations for all radionuclides from a single low-dimensional space. In this setting, an input sample is defined by the set of spectral signatures of all radionuclides for each sphere thickness. The IAE architecture is basically identical to that described above. For the first hidden layer of the encoder, the filter depth is 1 for the individual model and the number of radionuclides for the joint model. The same applies to the last decoder layer. All other layers remain unchanged.

III. Semi-blind Spectral unmixing (SEMSUN)

IAE models are integrated into an unmixing procedure to jointly estimate spectral signatures $X \in \mathbb{R}^{M\times N}$ and the counting vector $a \in \mathbb{R}^N$ from the observed spectrum $y \in \mathbb{R}^M$. For this purpose, a novel hybrid unmixing algorithm is developed by combining IAE models with the classical statistical approach. Two algorithm versions are presented, corresponding to the two IAE models described above.

Since $y \sim \mathcal{P}(Xa)$, we can calculate the likelihood function and define the cost function as negative log-likelihood. Mini-

mizing the negative log-likelihood is equivalent to minimizing the divergence:

$$D(y||Xa) = \sum_{m=1}^{M}((Xa)_m - y_m + y_m log(y_m) - y_m log((Xa)_m)) \quad (1)$$

In the present work, the problem of estimating X and a is expressed as follows:

$$\hat{X}, \hat{a} = \underset{X,a}{\text{Argmin}} \sum_{i=2}^{N} \chi_{\phi_i}(X_i) + \chi_{(.\geq 0)}(a) + D(y||Xa) \quad (2)$$

where $\chi_{(.\geq 0)}(a)$ stands for the positivity constraint on the vector a (i.e. vector with non-negative elements). $\chi_{\phi_i}(X_i)$ represents the constraint for each radionuclide: the spectral signature must be the decoding of the linear interpolation of the encoded anchor points.

$$\chi_{\phi_i}(X_i) = \begin{cases} 0 & \exists \lambda \in S_d : X_i = \Psi(\mathbf{\Omega}\lambda) \\ +\infty & \text{otherwise.} \end{cases}$$

i begins at 2 because the first column of the X matrix is the natural background Bkg and is already known, so there is no need to estimate it.

The problem is non-convex, but is approximately multi-convex (i.e. convex when X is fixed and approximately convex when a is fixed), it can be solved by the Block coordinate descent (BCD) algorithm [7]. The key idea of this algorithm is to divide the problem into several blocks. For each block, only one parameter is estimated, while the other parameters are fixed.

A. Semi-blind Spectral unmixing based on individual manifold learning (SEMSUN-i)

Constraints on the spectral signature can be defined using individual IAE models. $N-1$ models are trained to independently learn the shape and variability of the spectral signatures of $N-1$ radionuclides. In this case, BCD is used with N blocks: the first block estimates the a vector and the i^{th} block estimates the spectral signature of the i^{th} radionuclide. All blocks are executed consecutively until the algorithm converges. It is worth noting that this algorithm is effective when the radionuclides come from different source housings (e.g. the sphere thickness may be different for each radionuclide).

More precisely, at iteration $k+1$ for the first block, the non-negative vector a^{k+1} is estimated by minimizing the cost function when the matrix X^k is fixed:

$$a^{k+1} = \underset{a}{\text{Argmin}}\, \chi_{(.\geq 0)}(a) + D(y||X^k a) \quad (3)$$

Different algorithms have been proposed to solve this problem, such as the multiplicative update algorithm NNPU [1] or the Chambolle-Pock algorithm [2]. In this work, the NNPU is applied as it is faster.

Let: $X^{k,i} = (X_{Bkg}, X^{k+1}_{<i}, X^k_i, X^k_{>i})$ and $z_i = X^{k,i}a^{k+1} - X^k_i a^{k+1}_i$. For the i^{th} block, the estimated spectral signature of the i^{th} radionuclide is obtained by searching for the spectral signature that minimizes the cost function and satisfies the constraint based on the IAE model:

$$X_i^{k+1} = \underset{X_i}{\text{Argmin}}\, D(y||z_i + X_i a_i^{k+1}) + \chi_{\phi_i}(X_i) \quad (4)$$

The change of variable on X_i is carried out to overcome this problem:

$$X_i^{k+1} = \Psi(\mathbf{\Omega}\hat{\lambda}) \; with \; \hat{\lambda} = \underset{\lambda \in S_d}{\text{Argmin}}\, D(y||z_i + \Psi(\mathbf{\Omega}\lambda)a_i^{k+1})) \quad (5)$$

The task is simply to find the spectral signature generated by the IAE model that minimizes the cost function. It is noteworthy that using the IAE model to constrain spectral signatures is equivalent to using the IAE model as a generative model for our application. To deal with this optimization problem, SLQSP from Scipy [8] is used to consider constraint (simplex) on the latent variable λ. The SLSQP optimizer is a sequential least squares programming algorithm that replaces the original problem with a sequence of quadratic problems and transforms it into a least squares problem.

The stopping criterion is either the relative error on the counting a and spectral signatures X is less than a predefined value (default $1e^{-6}$), or the number of iterations is greater than the maximum number of iterations (default 200). The initial spectral signature and counting are set by the user.

B. Semi-blind Spectral unmixing based on joint manifold learning (SEMSUN-j)

When all the radionuclides are in the same source housing, the joint IAE model is more appropriate. In this scenario, a single IAE model can represent the spectral variability of all radionuclides. Consequently, the BCD algorithm is applied in two blocks: one for a and one for X. The first block is identical to the previous case. The second block searches for the spectral signatures of all radionuclides X generated by the IAE model that minimize the cost function :

$$\begin{aligned} &X^{k+1} = \Psi(\mathbf{\Omega}\hat{\lambda}) \\ &with \; \hat{\lambda} = \underset{\lambda \in S_d}{\text{Argmin}}\, D(y||X_{Bkg}a_1^{k+1} + \Psi(\mathbf{\Omega}\lambda)a_{i>1}^{k+1}) \end{aligned} \quad (6)$$

Detailed implementation is identical to that described above. The joint model looks for a single λ for all radionuclides instead of having a different λ value for each radionuclide, so the calculation time of the joint version is shorter. It should be noted that for both algorithms, convergence is not theoretically guaranteed. The assumption that, when a is fixed, the cost function is convex on X for the joint model or X_i for the individual model is not theoretically proven, as the IAE model is non-linear.

IV. Numerical evaluation of spectral unmixing of the hybrid algorithms

A. Data and Numerical evaluation

The datasets representing the deformations of the γ spectrum were obtained through MC simulations of radiation-matter interactions in a 3"×3" NaI(Tl) scintillation detector using Geant4 [5]. Four γ-emitting radionuclides: ^{57}Co, ^{60}Co,

^{133}Ba, ^{137}Cs covering a wide range of energies from 20 keV to 1600 keV were studied. The total number of spectral signatures for each radionuclide is 96. The NaI(Tl) detector's energy resolution was considered (6.5 keV at 662 keV).

For each radionuclide, 71 spectral signatures were randomly selected for training the IAE model and the remaining 25 for testing. The two anchor points are the spectral signatures corresponding to the smallest (1 μm) and largest thickness (30 mm). Another positivity constraint has also been added to the latent variable λ to define λ in $[0,1] \times [0,1]$ instead of $\mathbb{R} \times \mathbb{R}$. This constraint allows quick and efficient searching for the value of λ when using IAE as a generative model. The data and codes are available at the following link: https://github.com/triem1998/Gamma_spectrometry_SemSun.

The mixture of natural background (Bkg) and four radionuclides ^{57}Co, ^{60}Co, ^{133}Ba, ^{137}Cs with the corresponding mixing weights: 0.5, 0.08, 0.2, 0.12 0.1 was studied. The theoretical spectral signatures to be estimated correspond to a thickness of 5.2 mm of steel sphere for all radionuclides. The initial spectral signatures correspond to a thickness of 0.001 mm. The full-spectrum total counting is 2500. 1000 MC γ-spectra were simulated according to the Poisson distribution. The theoretical spectral signatures X and an example of simulated spectra are given in and Fig. 3 and Fig. 4.

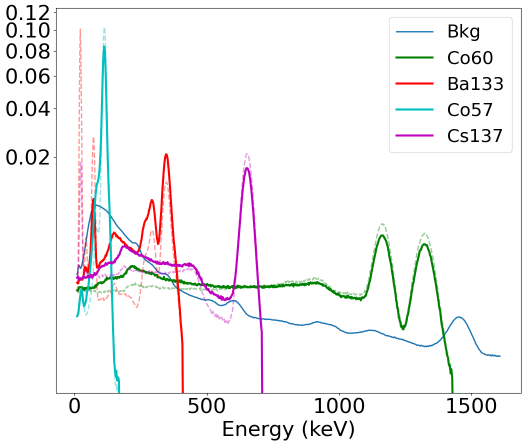

Fig. 3. Theoretical and initial spectral signatures X. The continuous curves correspond to the theoretical spectral signatures, and the dashed curves correspond to the initial ones.

B. Results

The results of the hybrid algorithms were compared with the non-negative estimation of X and a without additional constraints (blind spectral unmixing) performed by the non-negative matrix factorization (NMF) [9]. When X is assumed to be known, the NNPU algorithm is used to estimate a. In this case, the result is referred to as Oracle. The normalized mean square error (NMSE) is employed as a metric to evaluate the reconstruction performance of the estimated spectral signature:

$$\text{NMSE}(s,\hat{s}) = -10\log(\sum_m (s_m - \hat{s}_m)^2 / \sum_m (s_m)^2) \quad (7)$$

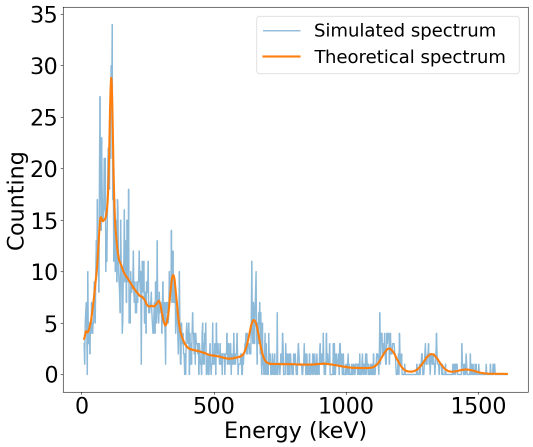

Fig. 4. An example of simulated spectrum y (right) with the total counting of 2500.

where $\hat{s}$ is the estimator of s.

Table I presents the NMSE of spectral signatures estimated for all algorithms. As anticipated, the spectral signatures are poorly estimated when using NMF, with very low NMSE values due to the absence of constraints on the spectral signatures. In this case, the problem is ill-posed, so the estimated spectral signatures are highly dependent on the initial spectral signatures. The SEMSUN-i result is better with a higher NMSE, but the values are relatively low for all radionuclides, particularly for ^{137}Cs with a median of around 14 dB. The best result is obtained with SEMSUN-j, which has the highest NMSE. The NMSE of ^{133}Ba is lower than that of the other radionuclides, as the spectral signature of ^{133}Ba is more sensitive to steel thickness (the variation is stronger). Fig. 5 and Fig. 6 show the spectral signature estimated with the SEMSUN-i and SEMSUN-j algorithms. The joint model's result is better because the joint model constrains the spectral signature from the same thickness, in contrast to the individual model.

Fig. 7 shows relative error distributions of the estimated counting for all radionuclides. The estimated counting of NMF is different from the expected values due to poor estimation of spectral signatures. SEMSUN-i yields a satisfactory estimation of the ^{133}Ba, ^{57}Co counting with the relative error distribution very close to that of Oracle. For ^{137}Cs, the relative error is around three times greater than the Oracle result. This result may be explained by the lower precision of the spectral signatures estimated by SEMSUN-i for this radionuclide. Concerning the SEMSUN-j results, the relative error distributions are similar to those of Oracle: the counting obtained when estimating spectral signatures is almost the same as in the case where spectral signatures are known.

V. Conclusion

A hybrid semi-blind unmixing approach has been developed for automatic full-spectrum analysis of γ-spectra that can

TABLE I

NMSE (dB) OF ESTIMATED SPECTRAL SIGNATURES OF ALL ALGORITHMS FOR ALL RADIONUCLIDES. THE VALUES IN EACH CELL ARE THE MEDIAN, 25TH PERCENTILE, AND 5TH PERCENTILE, RESPECTIVELY.

	^{60}Co	^{133}Ba	^{57}Co	^{137}Cs
SEMSUN-i	**18.4** |13.7, 11.9|	**19.7** |15.1, 10.0|	**21.6** |16.5, 12.0|	**14.1** |11.1, 8.6|
SEMSUN-j	**28.5** |24.1, 19.8|	**23.9** |19.1, 14.6|	**32.6** |28.7, 24.6|	**27.6** |22.8, 18.4|
NMF	**2.2** |2.0, 1.8|	**3.9** |3.5, 2.9|	**10.3** |9.6, 8.7|	**3.5** |3.2, 2.9|

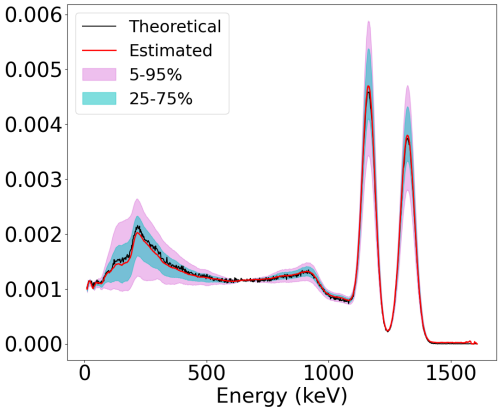

Fig. 5. ^{60}Co spectral signatures estimated by SEMSUN-i. Theoretical represents the theoretical spectral signature, and Estimated represents the average of the estimated spectral signatures for all MC simulated γ-spectra. 25-75 % represents the estimated signature between the 25 and 75 percentile. Same for 5-95%.

consider spectral deformation. As shown in this study, the IAE model is capable of learning the shape and variability of the spectral signature of all radionuclides with a limited dataset of simulated γ-spectra (less than 100). The BCD-based hybrid algorithm combining IAE models and MLE accurately accounts for spectral variability and Poisson statistics of the measurement. Numerical evaluation with a mixture of four radionuclides (^{57}Co, ^{60}Co, ^{133}Ba, ^{137}Cs) demonstrates the validity of this hybrid approach. Future work will extend this development to identifying radionuclides when their presence is unknown, using the model selection studied in [1] [2].

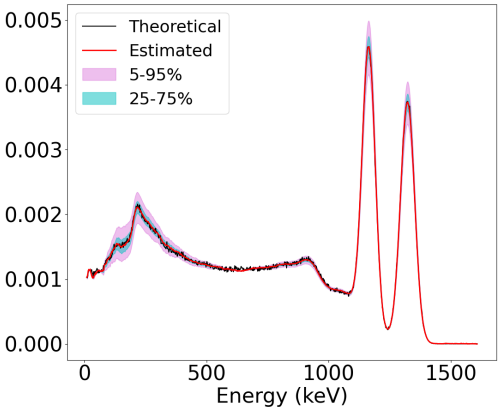

Fig. 6. Same as Fig. 5 with SEMSUN-j

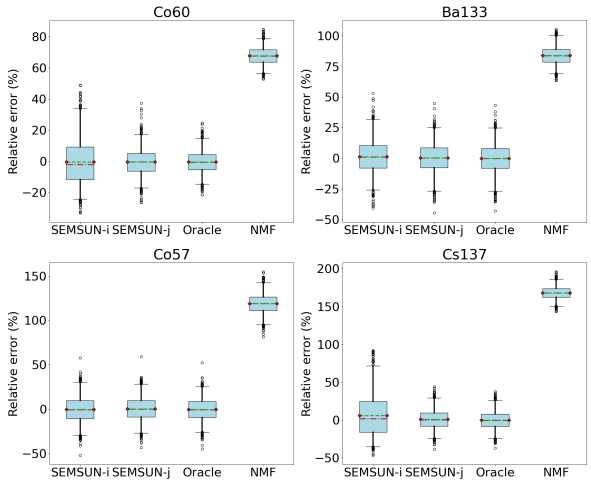

Fig. 7. Relative errors of estimated counting for all radionuclides. In the boxplot center, the red line is the median, and the blue line is the mean. The box is composed of the first and third quartiles. The whiskers represent the 2nd percentile and 98th percentile of the data.

REFERENCES

[1] R. André, C. Bobin, J. Bobin, J. Xu, and A. de Vismes Ott, "Metrological approach of γ-emitting radionuclides identification at low statistics: application of sparse spectral unmixing to scintillation detectors," *Metrologia*, vol. 58, no. 1, p. 015011, 2021.

[2] J. Xu, J. Bobin, A. de Vismes Ott, and C. Bobin, "Sparse spectral unmixing for activity estimation in γ-ray spectrometry applied to environmental measurements," *Applied Radiation and Isotopes*, vol. 156, p. 108903, 2020.

[3] F. M. de Oliveira, G. Daniel, and O. Limousin, "Artificial gamma ray spectra simulation using generative adversarial networks (gans) and supervised generative networks (sgns)," *Nuclear Instruments and Methods in Physics Research Section A: Accelerators, Spectrometers, Detectors and Associated Equipment*, vol. 1047, p. 167795, 2023.

[4] A. N. Turner, C. Wheldon, T. K. Wheldon, M. R. Gilbert, L. W. Packer, J. Burns, and M. Freer, "Convolutional neural networks for challenges in automated nuclide identification," *Sensors*, vol. 21, no. 15, p. 5238, 2021.

[5] S. Agostinelli, J. Allison, K. a. Amako, J. Apostolakis, H. Araujo, P. Arce, M. Asai, D. Axen, S. Banerjee, G. Barrand *et al.*, "Geant4—a simulation toolkit," *Nuclear instruments and methods in physics research section A: Accelerators, Spectrometers, Detectors and Associated Equipment*, vol. 506, no. 3, pp. 250–303, 2003.

[6] J. Bobin, R. C. Gertosio, C. Bobin, and C. Thiam, "An autoencoder-based model for learning regularizations in unmixing problems," *Digital Signal Processing*, p. 104058, 2023.

[7] Y. Xu and W. Yin, "A globally convergent algorithm for nonconvex optimization based on block coordinate update," *Journal of Scientific Computing*, vol. 72, no. 2, pp. 700–734, 2017.

[8] D. Kraft, "A software package for sequential quadratic programming," *Forschungsbericht- Deutsche Forschungs- und Versuchsanstalt fur Luft- und Raumfahrt*, 1988.

[9] D. Lee and H. S. Seung, "Algorithms for non-negative matrix factorization," *Advances in neural information processing systems*, vol. 13, 2000.